



ARL-TR-9097 • OCT 2020



Metabolic Modeling of *Pseudomonas putida* to Understand and Improve the Breakdown of Plastic Waste

by Leah A Lewis, Matthew A Perisin, and Alexander V Tobias

Approved for public release; distribution is unlimited.

NOTICES

Disclaimers

The findings in this report are not to be construed as an official Department of the Army position unless so designated by other authorized documents.

Citation of manufacturer's or trade names does not constitute an official endorsement or approval of the use thereof.

Destroy this report when it is no longer needed. Do not return it to the originator.



Metabolic Modeling of *Pseudomonas putida* to Understand and Improve the Breakdown of Plastic Waste

Leah A Lewis

Historically Black Colleges & Universities/Minority Institutions Summer Research Program, Hampton University

Matthew A Perisin and Alexander V Tobias

Sensors and Electron Devices Directorate, CCDC Army Research Laboratory

REPORT DOCUMENTATION PAGE			Form Approved OMB No. 0704-0188		
Public reporting burden for this collection of information is estimated to average 1 hour per response, including the time for reviewing instructions, searching existing data sources, gathering and maintaining the data needed, and completing and reviewing the collection information. Send comments regarding this burden estimate or any other aspect of this collection of information, including suggestions for reducing the burden, to Department of Defense, Washington Headquarters Services, Directorate for Information Operations and Reports (0704-0188), 1215 Jefferson Davis Highway, Suite 1204, Arlington, VA 22202-4302. Respondents should be aware that notwithstanding any other provision of law, no person shall be subject to any penalty for failing to comply with a collection of information if it does not display a currently valid OMB control number. PLEASE DO NOT RETURN YOUR FORM TO THE ABOVE ADDRESS.					
1. REPORT DATE (DD-MM-YYYY) October 2020		2. REPORT TYPE Technical Report		3. DATES COVERED (From - To) 1 June 2020–28 September 2020	
4. TITLE AND SUBTITLE Metabolic Modeling of <i>Pseudomonas putida</i> to Understand and Improve the Breakdown of Plastic Waste			5a. CONTRACT NUMBER		
			5b. GRANT NUMBER		
			5c. PROGRAM ELEMENT NUMBER		
6. AUTHOR(S) Leah A Lewis, Matthew A Perisin, and Alexander V Tobias			5d. PROJECT NUMBER		
			5e. TASK NUMBER		
			5f. WORK UNIT NUMBER		
7. PERFORMING ORGANIZATION NAME(S) AND ADDRESS(ES) CCDC Army Research Laboratory ATTN: FCDD-RLS-CB 2800 Powder Mill Rd Adelphi, MD 20783			8. PERFORMING ORGANIZATION REPORT NUMBER ARL-TR-9097		
9. SPONSORING/MONITORING AGENCY NAME(S) AND ADDRESS(ES) Department of Defense (DOD) Undersecretary for Research and Engineering (USRE) Historically Black Colleges and Universities/Minority-Serving Institutions (HBCU/MI) Summer Research Program			10. SPONSOR/MONITOR'S ACRONYM(S) DOD USRE HBCU/MI		
			11. SPONSOR/MONITOR'S REPORT NUMBER(S)		
12. DISTRIBUTION/AVAILABILITY STATEMENT Approved for public release; distribution is unlimited.					
13. SUPPLEMENTARY NOTES ORCID ID(s): Alexander V Tobias, 0000-0002-5866-5254; Matthew A Perisin, 0000-0003-3397-5296					
14. ABSTRACT Polyethylene terephthalate (PET) is the world's highest production-volume plastic and a major waste management issue for the Army. While synthetic polymers typically resist biodegradation, organisms have been discovered that can decompose PET into soluble but toxic monomers, ethylene glycol (EG) and terephthalic acid (TPA). <i>Pseudomonas putida</i> is a soil bacterium known for its receptiveness to genetic engineering and ability to metabolize an assortment of organic compounds. We sought to understand the pathways by which <i>P. putida</i> can metabolize EG and TPA. Our analyses employed two genome-scale metabolic models of <i>P. putida</i> KT2440: one on the web platform KBase and the other, COBRApy, implemented in Python. These models were used to generate flux balance analysis (FBA) output to quantitatively predict the organism's growth in different media. FBA results indicate that <i>P. putida</i> KT2440, described by the model iJN1463, is capable of biomass formation on EG and on protocatechuate (PCA), a metabolite two steps downstream of TPA. Most <i>P. putida</i> strains lack the protein machinery to import TPA and convert it to PCA. However, bioinformatic searches reveal homologous transporter proteins and enzymes in <i>P. putida</i> genomes that may be only a few mutational steps removed from performing the reactions for TPA metabolism.					
15. SUBJECT TERMS metabolic modeling, waste treatment, biodegradation, bioremediation, bioinformatics, computational biology					
16. SECURITY CLASSIFICATION OF:			17. LIMITATION OF ABSTRACT UU	18. NUMBER OF PAGES 33	19a. NAME OF RESPONSIBLE PERSON Alexander V Tobias
a. REPORT Unclassified	b. ABSTRACT Unclassified	c. THIS PAGE Unclassified			19b. TELEPHONE NUMBER (Include area code) (301) 394-4162

Contents

List of Figures	iv
List of Tables	v
Acknowledgment	vi
1. Introduction	1
1.1 Biological “Upcycling” of Plastics	1
1.2 Genome-Scale Metabolic Models and Flux Balance Analysis	2
2. Methods, Assumptions, and Procedures	4
3. Results and Discussion	5
3.1 KBase	5
3.2 COBRApy	6
3.3 SAMMlpy	7
3.4 Ethylene Glycol (EG) Metabolism	8
3.5 Protocatechuate (PCA) Metabolism	13
3.6 Protocatechuate (PCA) + Ethylene Glycol (EG) Metabolism	15
3.7 Terephthalate (TPA) Metabolism	15
4. Conclusions	19
5. References	21
List of Abbreviations	24
Distribution List	25

List of Figures

Fig. 1	PET hydrolysis generates terephthalic acid (TPA) and ethylene glycol (EG).....	2
Fig. 2	Illustrative explanation of constraint-based metabolic modeling.	3
Fig. 3	A screenshot from KBase showing some of its available applications	6
Fig. 4	Biomass flux map for <i>P. putida</i> KT2440 model iJN463 on EG carbon source.....	8
Fig. 5	KBase FBA output summary values for <i>P. putida</i> KT2440 supplied with EG	9
Fig. 6	EG reactions and fluxes with iJN1463.....	11
Fig. 7	PET degradation pathways as described in Ref 19	12
Fig. 8	PCA reactions and fluxes with iJN1463	14
Fig. 9	Proteins involved in the import and conversion of TPA to PCA.....	16

List of Tables

Table 1	Growth medium composition used in this work.....	4
Table 2	Summary statistics for the two <i>P. putida</i> KT2440 models run in COBRApy.....	6
Table 3	Exchange fluxes for model iJN463 supplied with EG (active transport).....	10
Table 4	Exchange fluxes for model iJN463 supplied with EG (passive transport).....	10
Table 5	Exchange fluxes for model iJN463 supplied with PCA (34dzbz) or PCA + EG (same results).....	15
Table 6	Summary of BLAST search results for <i>Comamonas</i> and <i>Rhodococcus</i> proteins involved in TPA import and catabolism to PCA	18

Acknowledgment

Funding for Ms Lewis' summer internship was provided by the Department of Defense Undersecretary for Research and Engineering Historically Black Colleges and Universities/Minority-Serving Institutions Summer Research Program.

1. Introduction

1.1 Biological “Upcycling” of Plastics

Polyethylene terephthalate (PET) is the world’s most popular synthetic polymer by annual production mass.¹ PET is primarily used to make apparel and plastic beverage bottles. Single-use PET water bottles are among the largest constituents of deployed forces waste streams in the US Army.² Due to the difficulty and low payoff of recycling plastics in remote areas, the Army would sometimes incinerate plastic waste in “burn pits”. For health and environmental reasons, burn pits have been outlawed with few exceptions. Therefore, safe and effective ways of handling plastic waste remain a challenge for our deployed forces. If waste could be used by our deployed forces as a feedstock for the production of useful chemicals, materials, or energy, it could be converted from a burdensome liability into an asset that reduces logistical footprint or provides other tactical advantages. A biological process to break down PET would have a number of attractive attributes. Biobased processes tend to be safe, operate under mild conditions of temperature and pressure, and require lower energy inputs than many (thermo)chemical processes. In addition, metabolism of waste PET by natural or engineered organisms offers the possibility of converting it into chemicals, materials, or energy for our Soldiers, even in remote environments.

Research has demonstrated that several environmental species of *Pseudomonas* are able to degrade synthetic plastics with varying degrees of efficiency. Of the approximately 140 known species of *Pseudomonas*, *Pseudomonas putida* has demonstrated the ability to break down and metabolize a large assortment of organic and especially toxic aromatic compounds.³ *P. putida* is also well-suited for genetic engineering, and an extensive and growing list of genetic tools has been developed for it.⁴ The hardiness, metabolic flexibility, and the ease with which *P. putida* can be genetically modified make it the bacterium of choice for several bioremediation and bioprocessing applications.⁵

PET is synthesized from the polymerization of terephthalic acid (TPA) and ethylene glycol (EG)⁶ (Fig. 1). Because it contains a high proportion of aromatic rings in its backbone, PET is one of the more environmentally persistent plastics.⁷ However, the recent discovery⁷ and engineering^{8,9} of enzymes capable of hydrolyzing PET to TPA and EG have fueled interest in the possibility of utilizing microorganisms to break down waste PET to reduce its volume or even convert it into useful products or energy.⁷

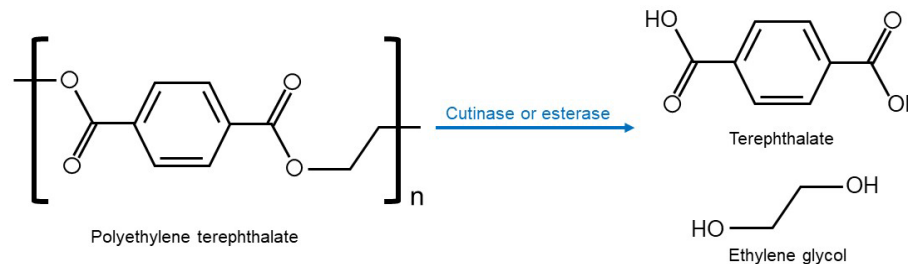


Fig. 1 PET hydrolysis generates terephthalic acid (TPA) and ethylene glycol (EG). (Figure based on Ref 10.)

For this summer undergraduate project, we focused on the second part of a potential bioprocess to break down PET: the metabolism of TPA and EG by *P. putida*. We took a genome-scale metabolic modeling approach to quantitatively investigate and assess the potential of this bacterium to grow on TPA and/or EG as the sole carbon sources.

Research has demonstrated that *P. putida* KT2440 possess all the genes necessary to form biomass on ethylene glycol.⁵ In addition, *P. putida* KT2440 has also displayed the ability to use ethylene glycol to produce energy.¹¹ We were interested in using genome-scale metabolic models of *P. putida* KT2440 to better understand its potential to grow on EG and/or TPA. We outlined several research questions to address in this project: Do different methods of constructing and analyzing these metabolic models produce different outputs? How do model outputs compare to experimental literature results? Can flux balance analysis (FBA) predict how well *P. putida* can grow on EG, TPA, or both? What do these models say about the viability of a bioprocess based on *P. putida* KT2440 to convert EG and TPA into benign biomass or even useful chemicals? And, could genetic modifications improve the ability of *P. putida* KT2440 to grow (produce biomass) on EG and/or TPA as the sole carbon sources?

1.2 Genome-Scale Metabolic Models and Flux Balance Analysis

A genome-scale metabolic model (GSMM) is a reconstruction of an organism's metabolism based on its sequenced and annotated genome.¹² An annotated genome identifies the enzymes an organism can express and the reactions they catalyze—namely their substrate(s) and product(s). This information is collected from published research about the organism and its enzymatic reactions. A genome-scale metabolic model is therefore a rich and interactive “knowledge base” about an organism that allows researchers to test hypotheses *in silico* in order to inform, focus, or better understand their experiments. The primary components of a GSMM are a table or matrix of all of the reactions carried out by the organism and a second table or matrix of all the compounds that participate in the reactions listed in the reactions

2. Methods, Assumptions, and Procedures

FBA models of *P. putida* KT2440 (KBase ID 19217/162098/1) were constructed in KBase¹⁴ at <https://www.kbase.us>. Minimal media files containing a single carbon source were generated and uploaded. Table 1 lists the medium file used with EG as the sole carbon source. Only the carbon source was changed when running FBAs with other sole carbon sources in KBase. For example, glucose minimal medium was used as a comparison benchmark. The composition of that medium was identical to the one in Table 1 except for the substitution of EG with glucose. The objective function for all FBAs run in this project was maximization of the biomass reaction flux. The biomass chemical formula was the KBase default Gram-negative biomass formula. Gap-filling was enabled and used by KBase to generate FBA outputs for *P. putida* KT2440 growing on EG.

Table 1 Growth medium composition used in this work

Compound ID	Compound name(s)	Concentration (mol/L)	Minimum flux (mmol [g cell dry mass] ⁻¹ h ⁻¹)	Maximum flux (mmol [g cell dry mass] ⁻¹ h ⁻¹)
cpd00992	Ethane-1,2-diol 1,2-Ethanediol Ethylene glycol	0.001	-100	20
cpd00013	NH ₄ plus NH ₄ ⁺ Ammonium Ammonia NH ₃	0.001	-100	5
cpd00009	Orthophosphoric acid Phosphoric acid Phosphate Orthophosphate	0.001	-100	5
cpd00048	SLF Sulfuric acid Sulfate	0.001	-100	5
cpd00063	Ca(2+) Ca ²⁺ Calcium	0.001	-100	100
cpd00099	Hydrochloride Hydrogen chloride Hydrochloric acid Chloride ion Cl ⁻ HCl Chloride	0.001	-100	100
cpd00149	Co ²⁺ Cobalt	0.001	-100	100
cpd00058	Copper Cu ⁺ Cu(I) Cu ¹⁺ Copper1 Cu(II) Cu ²⁺ Copper2	0.001	-100	100
cpd10515	Iron(2+) Ferrous ion Fe(II) Fe ²⁺	0.001	-100	100
cpd10516	Fe ³ Iron(3+) Ferric ion Fe(III) Fe ³⁺	0.001	-100	100
cpd00067	H ⁺	0.001	-100	100
cpd00001	OH ⁻ HO ⁻ Water H ₂ O	0.001	-100	100
cpd00205	K ⁺ Potassium	0.001	-100	100
cpd00254	Mg(2+) Mg Mg ²⁺ Magnesium	0.001	-100	100
cpd00030	Mn(III) Mn(II) Mn ²⁺ Manganese	0.001	-100	100
cpd00244	Ni ²⁺ Nickel	0.001	-100	100
cpd00971	Na ⁺ Sodium	0.001	-100	100
cpd00007	Dioxygen O ₂ Oxygen	0.001	-100	20
cpd00034	Zn(II) Zn ²⁺ Zinc	0.001	-100	100

Notes: For other sole carbon sources, only the first compound (EG) was changed. Compound IDs are for KBase.

Constraint-Based Reconstruction and Analysis Toolbox for Python (COBRApy)¹⁵ was run locally with the Anaconda3 Navigator Python interpreter. Training to learn the basics of Python scripting was through Software Carpentry.¹⁶ The tables comprising *P. putida* KT2440 metabolic reconstruction models iJN746 (2008)¹² and iJN1463 (2019)⁵ were obtained from the BiGG Models database¹⁷ at <http://bigg.ucsd.edu>.

The Semi-Automated Metabolic Map Illustrator in Python (SAMMIpy)¹⁸ was used to render FBA results obtained from COBRApy into metabolic pathway diagrams.

Basic Local Alignment Search Tool (BLAST) searches were run with the United States National Center for Biotechnology Information (NCBI) BLAST tool at <https://blast.ncbi.nlm.nih.gov>.

3. Results and Discussion

3.1 KBase

KBase¹⁴ was the first FBA modeling tool we used to predict the growth potential of *P. putida* KT2440 on carbon sources including ethylene glycol. KBase encompasses a web-based suite of “apps” (Fig. 3). Using these apps, we were able to load a public annotated genome for *P. putida* KT2440 (see Methods), construct a draft GSMM, and run flux balance analyses using various media files we created and uploaded to the system, such as the one in Table 1. Gap-filling was activated and required for this model of *P. putida* KT2440 to generate biomass flux on the medium listed in Table 1. Gap-filling is a KBase algorithm that reverses the direction of some reactions or adds additional reactions to KBase FBAs that otherwise would not generate biomass flux. This can be useful and informative as long as the user is aware and takes note of what reactions were reversed or added by the gap-filling algorithm. It is possible that gap-filling could generate physiologically unrealistic results. Because gap-filling was required for the *P. putida* KT2440 model to generate biomass flux on the EG medium listed in Table 1, this means the model did not originally contain all the metabolic reactions required for growth on EG. For this reason, as well as the availability of better-documented and experimentally validated models of *P. putida* KT2440 in the BiGG Models database,¹⁷ we transitioned our modeling efforts to the Python-based COBRApy modeling platform.

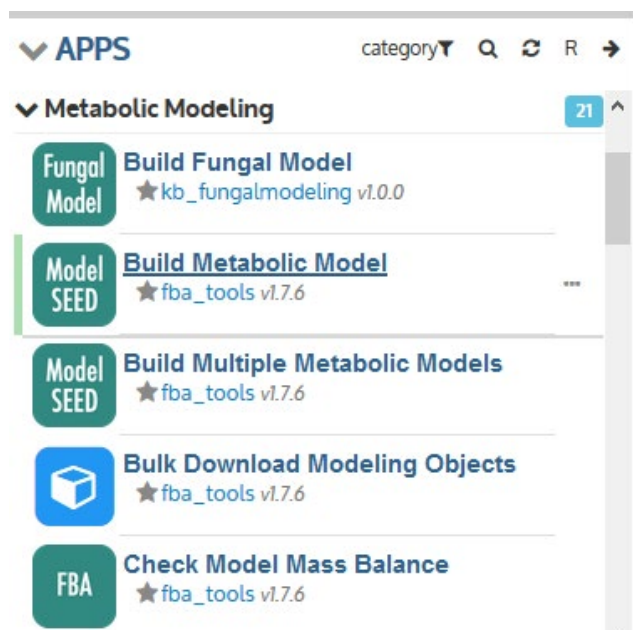


Fig. 3 A screenshot from KBase¹⁴ showing some of its available applications

3.2 COBRAPy

Constraint-Based Reconstruction and Analysis Toolbox for Python (COBRAPy)¹⁵ requires a Python interpreter. We used the Anaconda3 Navigator freeware. FBAs were performed with *P. putida* KT2440 metabolic reconstruction models iJN746,¹² published in 2008, and iJN1463,⁵ published in 2019, both by the Palsson group at UC San Diego (Table 2). The number in the name of each model corresponds to the number of genes it contains. “i” represents “in silico”, and JN are the initials of the primary model builder, Juan Nogales. Model iJN1463 is the newest and most detailed metabolic reconstruction of *P. putida* KT2440 and, like iJN746, was built for COBRAPy.

Table 2 Summary statistics for the two *P. putida* KT2440 models run in COBRAPy

BiGG ID	Organism	Metabolites	Reactions	Genes
iJN746	<i>P. putida</i> KT2440	907	1054	746
iJN1463	<i>P. putida</i> KT2440	2153	2927	1463

Neither model iJN1463 nor iJN746 is accessible through KBase. As summarized in Table 2, model iJN1463 contains many more genes, reactions, and metabolites than its predecessor, iJN746. Model iJN1463 includes pathways capable of generating biomass from a greater number of carbon and nitrogen sources. Model iJN1463 also generates more accurate and experimentally validated predictions of growth capabilities, growth rates, and flux distributions, and contains a more accurate and

detailed chemical formula for *P. putida* biomass.⁵ As mentioned in the Introduction, the chemical formula for biomass is an important aspect of a metabolic model and can substantially influence its outputs. This is another advantage of iJN1463 and COBRApy models more generally over KBase models, which only allow the user to choose among a few generic biomass formulas, such as one for Gram-negative bacteria.

Running FBA models with COBRApy does require learning the Python scripting language. Compared with the *P. putida* metabolic models available through KBase, the COBRApy-based models are better-documented with publications and much more extensively validated experimentally. In addition, COBRApy is a faster platform because users are able to run FBAs without uploading and downloading growth media and models each time. Unfortunately, KBase and COBRApy models are not able to run on the other platform because each type uses different data formats and notation. We conclude that, of the two platforms, COBRApy requires more investment to learn, but the investment is worthwhile because of all the benefits it offers.

3.3 SAMMIpy

We had hoped that SAMMIpy¹⁸ would be a useful tool to visualize the results (flux connectivities and magnitude) obtained from various FBAs through the metabolic network of *P. putida* KT2440, and therefore assist us in comparing the outputs of various models. SAMMIpy turned out to be a useful tool to visualize the connections between enzymes and metabolites involved in the metabolism of various carbon sources. We like how SAMMIpy visualizations can be filtered to show only the compounds and reactions directly involved in the metabolism of, for example, ethylene glycol. However, upgrades would make the tool more useful, such as the ability to display fluxes on standard metabolic maps (e.g., the tricarboxylic acid [TCA] cycle), more display options, and a clearer appearance to make the maps more suitable for inclusion in manuscript figures and presentation slides. Figure 4 shows a sample SAMMIpy visualization and plainly illustrates the tool's display shortcomings.

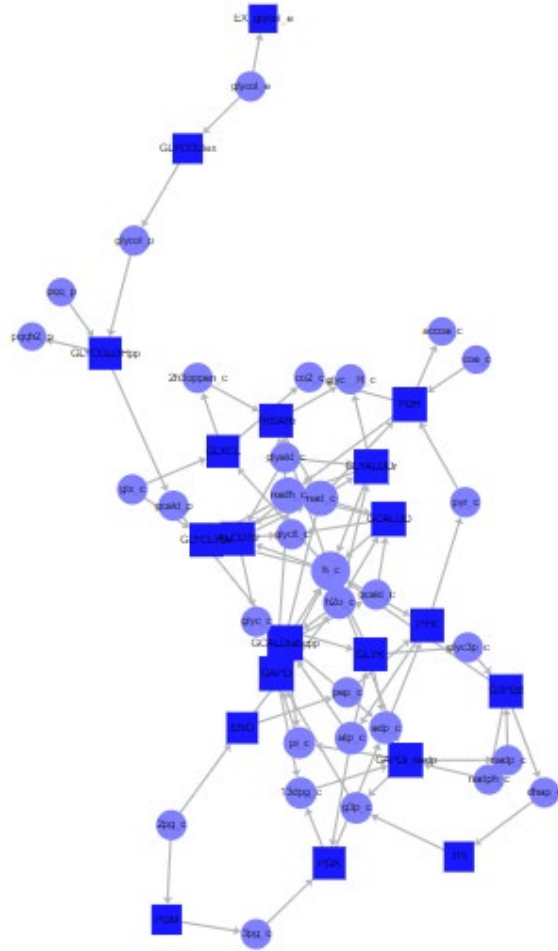


Fig. 4 Biomass flux map for *P. putida* KT2440 model iJN463 on EG carbon source. Map created with SAMMIpy.

3.4 Ethylene Glycol (EG) Metabolism

The first FBA results obtained with KBase model 19217/162098/1 of *P. putida* KT2440 predicted that biomass formation (growth) was possible on EG by a plausible route, with gap-filling activated. A biomass flux of 0.10 h^{-1} was obtained on EG (Fig. 5). For comparison, the biomass flux with identical inputs except glucose in the medium instead of EG as the sole carbon source was 0.46 h^{-1} for this KBase model of *P. putida* KT2440. It makes sense that maximum predicted biomass flux on EG is substantially lower than that on glucose, which is the preferred carbon source for many bacteria, including *P. putida*, as glucose catabolism requires fewer steps and yields more adenosine triphosphate (ATP) equivalents per gram.

v1 - KBaseFBA.FBA-13.2	
Overview Reaction fluxes Exchange fluxes Genes Biomass Pathways Bar charts	
Details	
ID	leahlewis.narrative_1591626649309/Pputida_EG2.gf.0
Object type	KBaseFBA.FBA-13.2
Owner	leahlewis
Version	1
Mod-date	2020-06-08T14:34:36+0000
Objective value	0.101946
Model	Pputida_EG2
Media	EthGlycol_Min_Med_TSV.tsv_media
Single KO	0
Number reactions	602
Number compounds	26
Gene KO	0
Reaction KO	0
Custom bounds	0
Custom constraints	0
Media supplements	0

Fig. 5 KBase FBA output summary values for *P. putida* KT2440 supplied with EG

With COBRAPy, *P. putida* KT2440 model iJN1463 was able to grow (produce biomass) on ethylene glycol, while model iJN746 could not. Model iJN1463 includes many additional reactions and other enhancements over previous models of KT2440. Additionally, EG metabolism was explicitly validated experimentally as part of the construction of iJN1463.⁵ In that study, the authors found that it took a full 48 h for *P. putida* KT2440 to begin growing on EG as the sole carbon source, which is longer than prior tests that concluded “no growth” were run.

We obtained a biomass flux on EG of 0.269 h^{-1} with iJN1463. As a benchmark, we obtained a biomass flux of 0.53 h^{-1} for iJN1463 provided with identical inputs except for glucose as the sole carbon source. The model predicted output exchange fluxes from EG metabolism were water, carbon dioxide, and protons (Table 3). When analyzing the pathway by which EG is metabolized by iJN1463, a possible genetic engineering opportunity was uncovered. The pathway includes a step where glycolaldehyde is actively imported from the periplasm to the cytoplasm with concurrent consumption of a molecule of ATP. If this active, energy-consuming step could be substituted with a passive transport step that does not consume ATP, the predicted growth potential of iJN1463 on EG should increase due to the energy conserved. Expression of a passive transport protein for EG is within the realm of possibilities of straightforward genome editing of *P. putida*. We ran another FBA with a passive EG import reaction added to iJN1463. This allowed the active transport of glycolaldehyde from the periplasm to the cytoplasm to be bypassed. The resulting model’s output predicted a biomass flux on EG of 0.413 h^{-1} if passive transport were utilized (Table 4).

Table 3 Exchange fluxes for model iJN463 supplied with EG (active transport)

IN_FLUXES		OUT_FLUXES		OBJECTIVES	
ID	FLUX	ID	FLUX	ID	FLUX
o2_e	10	h2o_e	21.7	BIOMASS_KT2440_WT3	0.269
glycol_e	8.51	co2_e	6.19		nan
nh4_e	2.86	h_e	2.63		nan
pi_e	0.247		nan		nan

Note: nan: no flux.

Table 4 Exchange fluxes for model iJN463 supplied with EG (passive transport)

IN_FLUXES		OUT_FLUXES		OBJECTIVES	
ID	FLUX	ID	FLUX	ID	FLUX
etglycol_e	10	h2o_e	24.2	BIOMASS_KT2440_WT3	0.413
o2_e	7.7	h_e	4.04		nan
nh4_e	4.39	co2_e	3.38		nan
pi_e	0.38		nan		nan

Note: nan: no flux.

SAMMIpy was used to visualize the network of enzymes and metabolites involved in the catabolism of EG by model iJN1463 (Fig. 4). However, because the maps generated with SAMMIpy did not display flux values and are generally difficult to decipher, we drew a pathway map that illustrates the reactions and their fluxes calculated with COBRAPy, along with the structures of the metabolites (Fig. 6). The map clearly shows the active transport step (#3) where ATP is consumed. Furthermore, the large number of steps (18) involved in the metabolism of EG to acetyl-CoA exemplifies the challenge of utilizing EG as the sole carbon source and helps explain why the biomass flux was lower on EG than on glucose (10–11 steps to acetyl-CoA). Notably, the pathway from EG to acetyl-CoA generated by COBRAPy with iJN1463 differs from the one shown in Fig. 7 from Ref 19. In reality, each pathway diagram represents an “excerpt” or “filtered view” of a metabolic network, and the main difference between the two pathway maps lies perhaps in different choices of metabolites and reactions to emphasize after glyoxylate. Also, the pathway depicted in Fig. 7 is not necessarily for *P. putida*. Because COBRAPy provided flux values for each reaction, our pathway diagram in Fig. 6 shows the highest flux path from every node (metabolite).

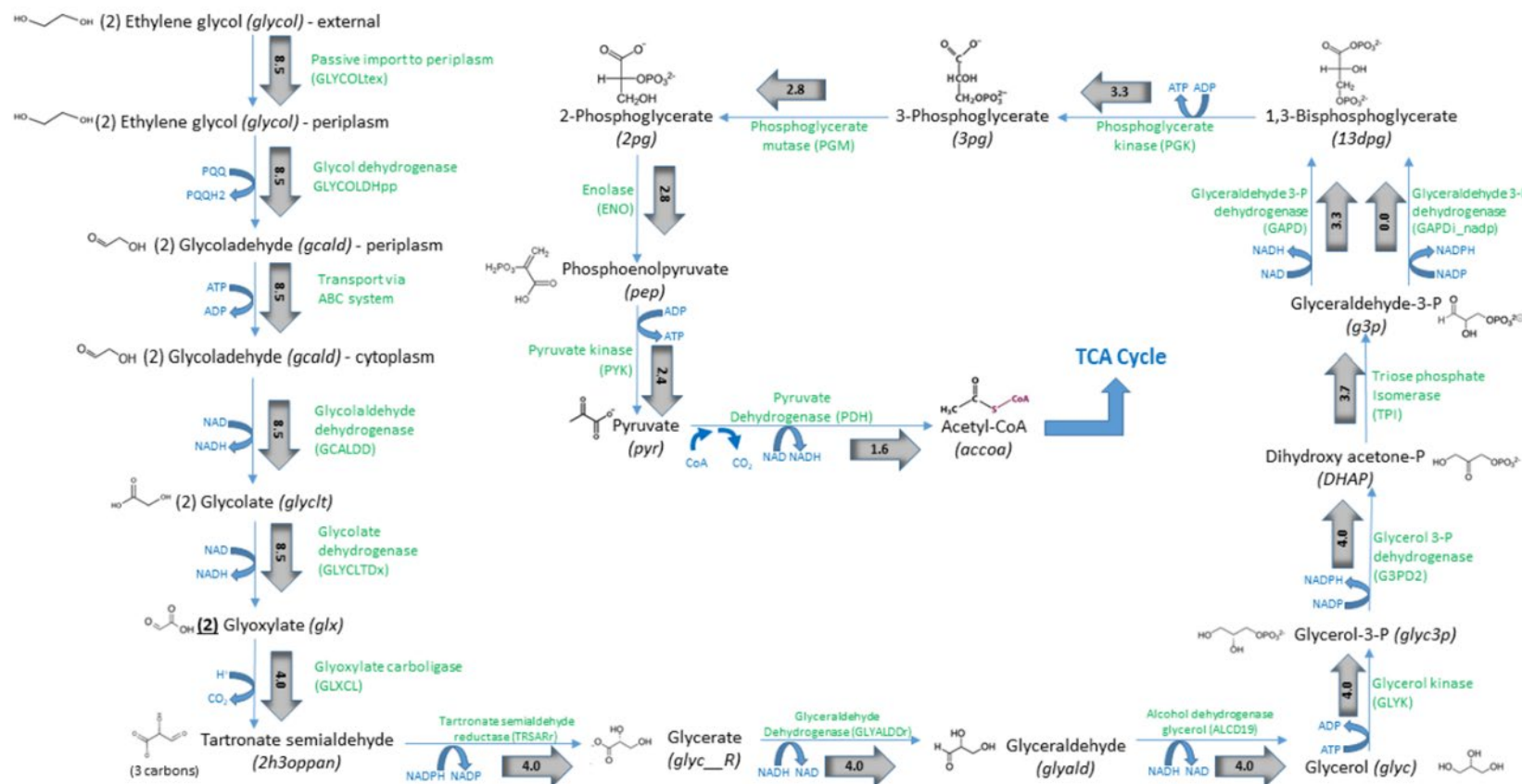


Fig. 6 EG reactions and fluxes with iJN1463. Flux values for each step are shown inside the gray arrows and are in units of $\text{mmol (g cell dry mass)}^{-1} \text{h}^{-1}$. Flux values decrease at certain steps where a metabolite participates in other reactions not shown. Bracketed terms in black are the official BiGG/COBRapy names for each metabolite; bracketed terms in green are the official BiGG/COBRapy names for each enzyme.

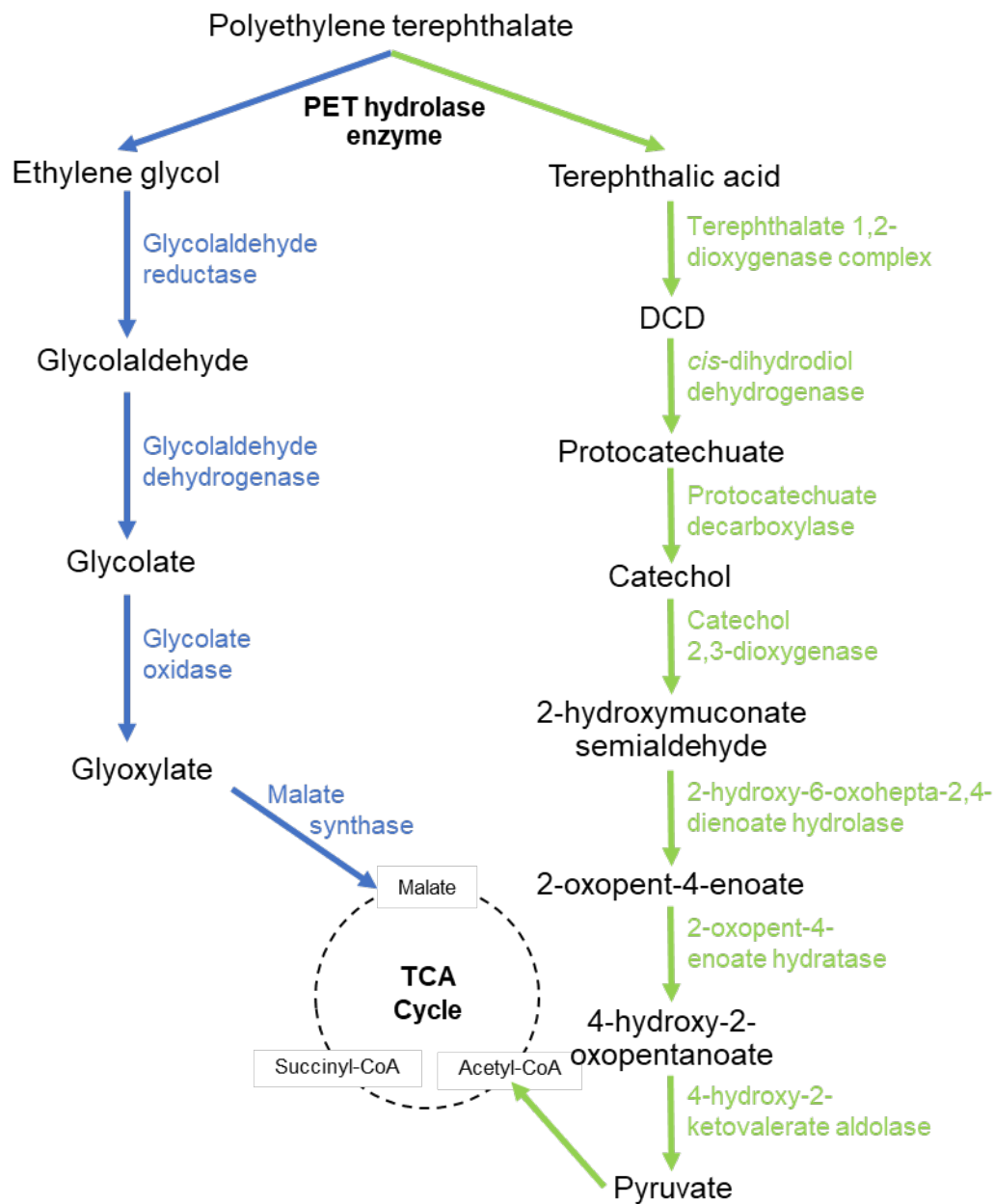


Fig. 7 PET degradation pathways as described in Ref 19. After hydrolysis of the polymer, degradation of the soluble monomers ethylene glycol and terephthalic acid proceeds along two separate pathways. Our FBA models yielded several differences in both pathways (Figs. 6 and 8). DCD: 1,2-dihydroxy-3,5-cyclohexadiene-1,4-dicarboxylate. TCA: tricarboxylic acid.

3.5 Protocatechuate (PCA) Metabolism

In addition to EG, TPA is produced as a monomer of PET hydrolysis. However, neither iJN1463 nor the entire BiGG database contains an entry for TPA. The closest metabolite downstream of TPA with a BiGG database entry is protocatechuate (PCA, see Fig. 7), which is two reaction steps from TPA.¹⁹ Since PCA is present in iJN1463, we first focused our study of TPA metabolism by *P. putida* on the steps after PCA.

If FBA of iJN1463 provided with PCA as the sole carbon source in the medium has a positive biomass flux, then at most, it might lack a TPA transporter protein and the two enzymes that convert TPA to PCA (TPA dioxygenase and *cis*-dihydrodiol dehydrogenase). Since these transporters and enzymes are known to be present in other microbes, it should be relatively facile to insert an expression cassette for them into the *P. putida* genome. This was actually performed by Beckham and coworkers,²⁰ who found that *P. putida* KT2440 could grow well on PCA but could not grow on TPA without the additional expression of a heterologous TPA transporter, a TPA dioxygenase and a *cis*-dihydrodiol dehydrogenase (see Section 3.7).

Since iJN1463 was the only *P. putida* metabolic model that predicted growth (biomass flux) on EG, we focused on that model for the FBAs with PCA. In the BiGG/COBRApy nomenclature, PCA is “34dhbz” in reference to its more systematic name, 3,4-dihydroxybenzoate. iJN1463 did predict the possibility of growth on PCA, with a biomass flux of 0.289 h⁻¹ (Table 5). Figure 8 is a pathway map for PCA catabolism by iJN1463. Note that the pathways depicted in Figs. 6 and 8 are quite different from each other. The PCA-to-acetyl-CoA pathway shown in Fig. 8 consists of eight steps, which is much shorter than the 18-step EG-to-acetyl-CoA pathway of Fig. 6. In addition, the transmembrane-transport steps for the PCA pathway are all passive (do not require consumption of ATP or ATP equivalents).

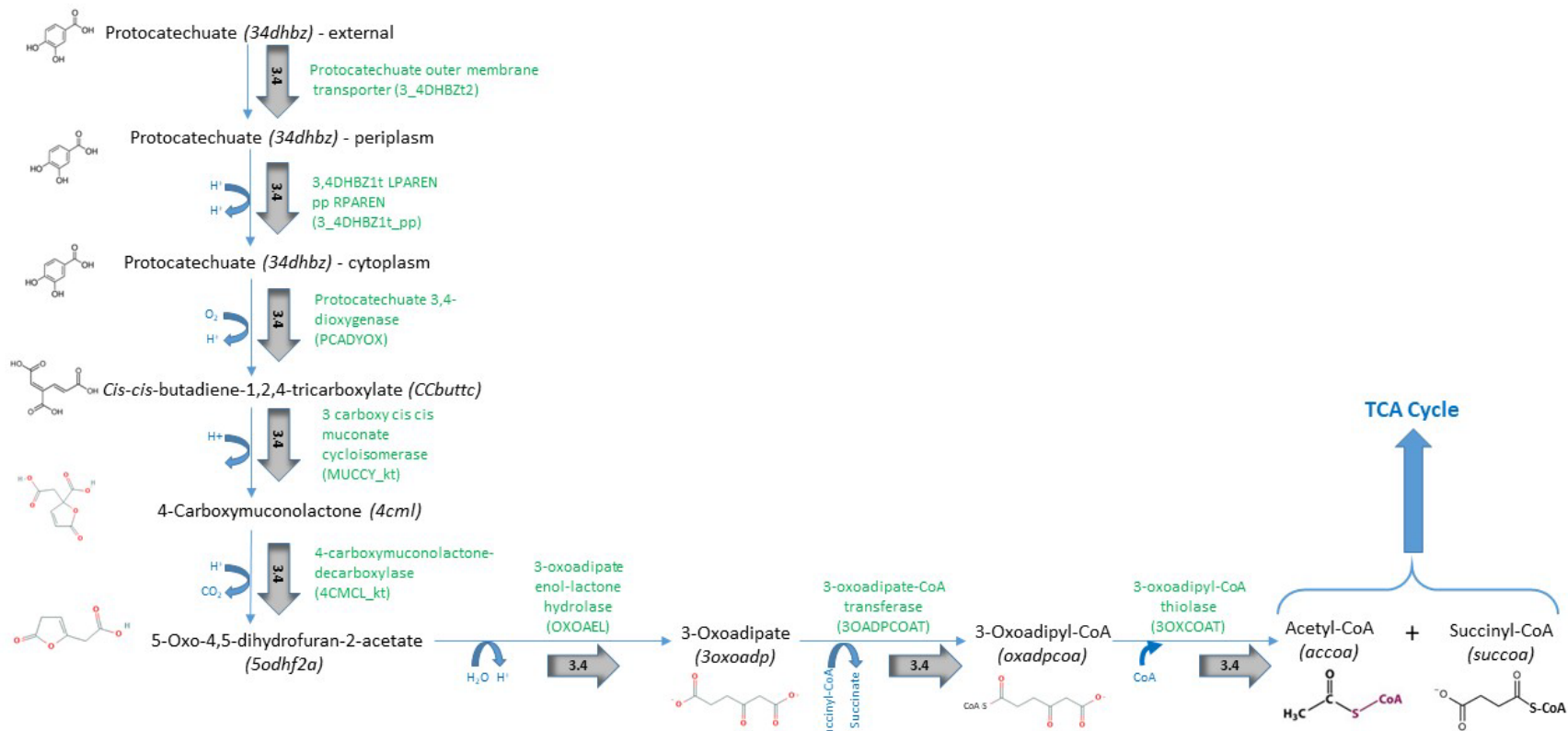


Fig. 8 PCA reactions and fluxes with iJN1463. Flux values for each step are shown inside the gray arrows and are in units of mmol (g cell dry mass)⁻¹ h⁻¹. Flux values decrease at certain steps where a metabolite participates in other reactions not shown. Bracketed terms in black are the official BiGG/COBRAPy names for each metabolite; bracketed terms in green are the official BiGG/COBRAPy names for each enzyme.

Table 5 Exchange fluxes for model iJN463 supplied with PCA (34dwbz) or PCA + EG (same results)

IN_FLUXES		OUT_FLUXES		OBJECTIVES	
ID	FLUX	ID	FLUX	ID	FLUX
o2_e	10	co2_e	12.2	BIOMASS_KT2440_WT3	0.289
34dwbz_e	3.4	h2o_e	6.15		nan
nh4_e	3.08		nan		nan
h_e	0.57		nan		nan
pi_e	0.266		nan		nan

Note: nan = no flux.

3.6 Protocatechuate (PCA) + Ethylene Glycol (EG) Metabolism

Because the complete degradation of PET would require the simultaneous consumption of TPA and EG, we performed another set of FBAs in which PCA and EG were provided in the medium as dual carbon sources. The biomass flux obtained for iJN1463 utilizing EG and PCA as dual carbon sources was the same biomass flux of 0.289 obtained previously with PCA alone (Table 5). Instead of consuming PCA and EG simultaneously, the FBA predicted that *P. putida* KT2440 would exhaust all PCA before transitioning to EG. While this is reminiscent of the “diauxic” metabolism commonly seen for bacteria provided with multiple sugars, (e.g., glucose and lactose), diauxic metabolism is controlled by complex genetic regulatory mechanisms. However, recall that FBA models contain no information about genetic regulation. Therefore, the FBA of iJN1463 provided with PCA and EG predicts PCA consumption exclusively simply because the biomass flux obtained on PCA alone (0.289 h^{-1}) is greater than that obtained on EG alone (0.269 h^{-1}), and the objective function of the FBA is biomass flux maximization. Some type of “synergy” would be required for an FBA model to predict co-utilization of multiple carbon sources with unequal individual objective fluxes, such as improved redox balance if both substrates are metabolized. Results like these show why it is best to be skeptical of FBA-based predictions. Experimental confirmation is important, both to validate predictions and also to help improve the accuracy of models.

3.7 Terephthalate (TPA) Metabolism

Neither TPA nor reactions involving TPA are present in the BiGG database, nor is TPA mentioned in metabolic modeling publications involving *P. putida*, at least to our knowledge. We could manually add the transport and enzyme conversion steps involved in conversion of extracellular TPA to intracellular PCA (Fig. 9). However, the connection of this exercise to reality would remain tenuous without additional evidence. Two publications in the literature are important to discuss here. Beckham

and colleagues at the National Renewable Energy Laboratory of the US Department of Energy recently published in a patent application that *P. putida* KT2440 does not contain a complete TPA catabolic pathway or the proteins required to transport TPA into the cell.²⁰ They expressed the genes *tphC* and *tpiBA* from *Comamonas* sp. strain E6,²¹ which encode a tripartite tricarboxylate-type TPA transporter complex, or *tpaK* from *Rhodococcus jostii* RHA1, which encodes a major facilitator superfamily-type TPA transporter.²² In addition, Beckham et al. co-expressed either of two TPA-to-PCA catabolic operons from *Comamonas* sp. E6²³ or an analogous TPA-to-PCA operon from *R. jostii* RHA1.²² They found that the combination of *tpaK* and either of the TPA-to-PCA operons from *Comamonas* sp. E6 enabled growth of engineered *P. putida* KT2440 on TPA as the sole carbon source.²⁰

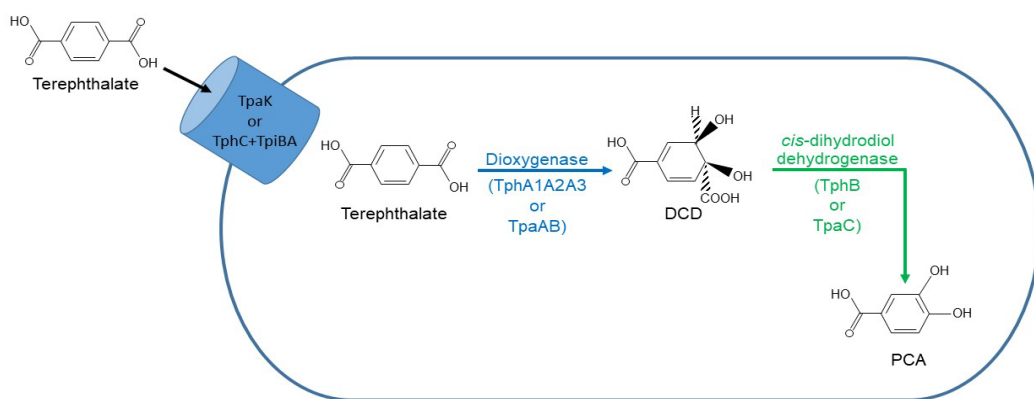


Fig. 9 Proteins involved in the import and conversion of TPA to PCA. TpaK: TPA transport protein from *Rhodococcus*. TphC+TpiBA comprise the three-part TPA permease from *Comamonas*. TphA1A2A3 comprise the *Comamonas* TPA 1,2-dioxygenase. TpaAB: *Rhodococcus* TPA 1,2-dioxygenase; TphB: cis-dihydrodiol dehydrogenase from *Comamonas*; TpaC: cis-dihydrodiol dehydrogenase from *Rhodococcus*; DCD: 1,2-dihydroxy-3,5-cyclohexadiene-1,4-dicarboxylate.

The second significant finding comes from Kenny and coworkers, who discovered two *P. putida* isolates from soil, GO16 and GO19, that are able to grow on TPA as the sole carbon and energy source.²⁴ To our knowledge, the genomes of GO16 and GO19 have not been sequenced, although a follow-up publication from the same group that describes processes for converting PET to bio-derived polyhydroxyalkanoate polymers using strain GO16 was very recently published as a preprint.²⁵ These results suggest that although most strains of *P. putida* likely do not possess the complete set of proteins and enzymes to import and convert TPA to PCA, *P. putida* may harbor a sufficiently similar complement of proteins and enzymes such that only a small number of mutations would be required to convert them into a functional TPA-to-PCA pathway. To assess this possibility, we utilized the Basic Local Alignment Search Tool (BLAST)²⁶ to search for homologs of

Rhodococcus or *Comamonas* TPA-to-PCA pathway proteins encoded in the *P. putida* genome (NCBI taxid: 136845).

The results of this BLAST analysis of known TPA catabolic proteins against *P. putida* sequences are summarized in Table 6. For all the proteins, a close homolog in *P. putida* was found. The annotations of these homologs indicate very similar functions and identical chemical mechanism, with possible differences in (known) substrate specificity. It is therefore not difficult to envision how a small number of specificity-altering mutations in TPA pathway homologs such as those listed in Table 6 could have enabled *P. putida* environmental strains GO16 and GO19 to grow on TPA.

Table 6 Summary of BLAST search results for *Comamonas* and *Rhodococcus* proteins involved in TPA import and catabolism to PCA. See Fig. 9 for additional information.

Function	Protein	Description	Species and NCBI accession number	Closest homolog in <i>P. putida</i> group (taxid: 136845) and NCBI accession number	% identity of closest homolog	Comments
TPA import	TpaK	MFS transporter	<i>R. jostii</i> RHA1, WP_011599113.1	MFS transporter, WP_103444220.1	70	Indicates <i>P. putida</i> possesses an MFS transporter
	TphC	TPA permease, TTT substrate-binding protein	<i>Comamonas testosteroni</i> , AAX18940.1	TTT substrate-binding protein, WP_064303473.1	35	The TTT substrate-binding protein is the portion of the TTT complex responsible for ligand specificity
Oxidation	TpaAa	Large subunit of ring-hydroxylating 1,2-dioxygenase system	<i>R. jostii</i> RHA1, ABG99221.1	Rieske 2Fe-2S domain-containing protein, WP_103444217.1	77	Next-closest match is 44%, large subunit of aromatic dioxygenase (CAE92855.1)
	TphA2	Large subunit of ring-hydroxylating 1,2-dioxygenase system	<i>Comamonas</i> sp. E6, BAE47085.1		69	
Dehydrogenation	TpaC	DCD (terephthalate dihydrodiol) dehydrogenase	<i>R. jostii</i> RHA1, ABG99223.1	4-hydroxythreonine-4-phosphate dehydrogenase, PdxA WP_103444218.1	68	TphB known to be a member of PdxA dehydrogenase family ²⁷
	TphB	DCD (terephthalate dihydrodiol) dehydrogenase	<i>Comamonas</i> sp. E6, BAE47087.1		49	

Notes: BLAST searches were performed at <https://blast.ncbi.nlm.nih.gov/Blast.cgi>. MFS = major facilitator superfamily; TTT = tripartite tricarboxylate transporter.

As a path forward, it would be very interesting to acquire and test the TPA-metabolizing *P. putida* strains described in Refs. 20 and 24 in our laboratory. The opportunity to culture the engineered strains from Beckham and colleagues at the National Renewable Energy Laboratory and the environmental strains from Kenny et al. on TPA, and to perform genome sequencing and transcriptomic analysis on them would very nicely complement and extend this modeling study. By comparing the engineered strains with the evolved ones, not just in terms of the rate of growth on TPA but also in terms of the genetic changes and quantitative patterns of gene expression, our understanding of TPA and EG metabolism by *P. putida* would be greatly expanded. To this end, the *P. putida* proteins identified and listed in Table 6 would serve as our initial guide to look for mutations in the environmental strains responsible for their gain of TPA catabolic function.

4. Conclusions

In this study, we performed an initial set of FBAs that contributed to our understanding of the possibility of utilizing the bacterium *Pseudomonas putida* to break down the soluble monomers comprising PET plastic: EG and TPA. Our analyses with genome-scale metabolic model iJN1463 of *P. putida* KT2440 showed that growth on EG is possible and could yield a biomass flux approximately half that achievable on glucose. Terephthalic acid was not part of the iJN1463 model, and literature implies that *P. putida* lacks the protein machinery to import it and convert it to PCA. Model iJN1463 does indicate that *P. putida* KT2440 can metabolize and grow on PCA.

Our attempt to model the simultaneous metabolism of EG and PCA did not lead to much insight, as the FBA, with our input objective of maximizing biomass flux, simply predicted that *P. putida* KT2440 would consume PCA only if both PCA and EG were supplied in the growth medium. Since this prediction was made by a model that includes no information on thermodynamics, kinetics, or genetic regulation (as is the case for all FBA models), this result should be taken with a grain of salt.

There are some strains of *P. putida* described in the literature reported to be capable of TPA catabolism.^{20,24} To continue our study of microbial metabolism of PET monomers, especially TPA, an attractive next step would be to obtain these published strains for our own testing, evaluation, and analysis in the laboratory. For environmentally evolved strains GO16 and GO19,²⁴ whose molecular mechanisms of TPA import and catabolism remain obscure and possibly unexplored, genome sequencing and transcriptomic analysis might unravel how these strains evolved to be able to grow on TPA. We suspect that mutations in some of the *P. putida* genes

encoding proteins listed in Table 6 could be responsible for this potentially useful phenotype.

Relying on a single microorganism to metabolize both the EG and TPA present in PET hydrolysate may prove less efficient than a mixed consortium of EG-metabolizing and TPA-metabolizing “specialists”. With such consortia, maintaining a stable and desirable balance of each organism can be a challenge.²⁸ For this application, each specialist could potentially be a strain of *P. putida*. This could avoid the need for compromises in fermentation conditions that are sub-optimal for the individual organisms. The EG specialist could be one of a number of known *P. putida* strains, and a collection of such strains could be evaluated for this purpose. The TPA specialist could be an engineered or evolved strain of *P. putida* with a key early EG pathway protein knockout. Each specialist strain would have its own niche in the fermentation system, and the independence of their nutrition sources could produce a stable, “neutralistic”²⁸ consortium.

5. References

1. Conant JM. US Army lab finds plastic bottles, other waste products have re-use potential for battlefield. US Army; 2018 Mar 28 [accessed 2020 Oct 13]. https://www.army.mil/article/202398/us_army_lab_finds_plastic_bottles_other_waste_products_have_re_use_potential_for_battlefield.
2. Preston B. Attack of the warzone water bottles. State of the Planet. 2011 May 16 [accessed 2020 Oct 13]. <https://blogs.ei.columbia.edu/2011/05/16/attack-of-the-warzone-water-bottles/>.
3. Wilkes R, Aristilde L. Degradation and metabolism of synthetic plastics and associated products by *Pseudomonas* sp.: capabilities and challenges. J Appl Microbiol. 2017;123(3):582–593.
4. Cook TB, Rand JM, Nurani W, Courtney DK, Liu SA, Pflieger BF. Genetic tools for reliable gene expression and recombineering in *Pseudomonas putida*. J Indust Microbiol Biotechnol. 2018;45(7):517–527.
5. Nogales J, Mueller J, Gudmundsson S, Canalejo FJ, Duque E, Monk J, Feist AM, Ramos JL, Niu W, Palsson BØ. High-quality genome-scale metabolic modelling of *Pseudomonas putida* highlights its broad metabolic capabilities. Environ Microbiol. 2019;22(1):255–269.
6. Salvador M, Abdulmutalib U, Gonzalez J, Kim J, Smith AA, Faulon J-L, Wei R, Zimmermann W, Jimenez JI. Microbial genes for a circular and sustainable Bio-PET economy. Genes. 2019;10(5):373.
7. Yoshida S, Hiraga K, Takehana T, Taniguchi I, Yamaji H, Maeda Y, Toyohara K, Miyamoto K, Kimura Y, Oda K. A bacterium that degrades and assimilates poly(ethylene terephthalate). Science. 2016;351(6278):1196–1199.
8. Son HF, Cho IJ, Joo S, Seo H, Sagong HY, Choi SY, Lee SY, Kim K-J. Rational protein engineering of thermo-stable PETase from *Ideonella sakaiensis* for highly efficient PET degradation. ACS Catalysis. 2019;9:3519–3526.
9. Furukawa M, Kawakami N, Tomizawa A, Miyamoto K. Efficient degradation of poly(ethylene terephthalate) with *Thermobifida fusca* cutinase exhibiting improved catalytic activity generated using mutagenesis and additive-based approaches. Sci Rep. 2019;9:16038.
10. iGEM. Degradation. Technische Universitat Darmstadt; 2012 [accessed 2020 Oct 13]. http://2012.igem.org/Team:TU_Darmstadt/Project/Degradation.

11. Franden MA, Jayakody LN, Li W, Wagner NJ, Cleveland NS, Michener WE, Hauer B, Blank LM, Wierckx N, Klebensberger J, Beckham GT. Engineering *Pseudomonas putida* KT2440 for efficient ethylene glycol utilization. *Metab Eng.* 2018;48:197–207.
12. Nogales J, Palsson BØ, Thiele I. A genome-scale metabolic reconstruction of *Pseudomonas putida* KT2440: iJN746 as a cell factory. *BMC Syst Biol.* 2008;2:79.
13. Orth JD, Thiele I, Palsson BØ. What is flux balance analysis? *Nat Biotechnol.* 2010;28(3):245–248.
14. Arkin AP, Cottingham RW, Henry CS, Harris NL, Stevens RL, Maslov S, Dehal P, Ware D, Perez F, Canon S, et al. KBase: The United States Department of Energy systems biology knowledgebase. *Nat Biotechnol.* 2018;36(7):566–569.
15. Ebrahim A, Lerman JA, Palsson BØ, Hyduke DR. COBRApy: COntstraints-based reconstruction and analysis for Python. *BMC Syst Biol.* 2013;7:74.
16. Programming with Python [accessed 2020 June 15]. <https://swcarpentry.github.io/python-novice-inflammation/>.
17. King ZA, Lu JS, Dräger A, Miller PC, Federowicz S, Lerman JA, Ebrahim A, Palsson BØ, Lewis NE. BiGG models: a platform for integrating, standardizing, and sharing genome-scale models. *Nucleic Acids Res.* 2016;44: D515–D522.
18. Schultz A, Akbani R. SAMMI: a semi-automated tool for the visualization of metabolic networks. *Bioinformatics.* 2019;36(8):2616–2617.
19. iGEM. PlastiCure. Pasteur Institute; 2015 [accessed 2020 Oct 13]. http://2015.igem.org/Team:Pasteur_Paris/Description.
20. Beckham GT, Jayakody LN, Guss AM, Mand TD, Johnson CW, Pardo Mendoza I. Engineered microorganisms for the deconstruction of polymers. International patent application WO2019222396A1. 2019.
21. Hosaka M, Kamimura N, Toribami S, Mori K, Kasai D, Fukuda M, Masai E. Novel tripartite aromatic acid transporter essential for terephthalate uptake in *Comamonas* sp. strain E6. *Appl Environ Microbiol.* 2013;79(19):6148–6155.
22. Hara H, Eltis LD, Davies JE, Mohn W. Transcriptomic analysis reveals a bifurcated terephthalate degradation pathway in *Rhodococcus* sp. strain RHA1. *J Bacteriol.* 2007;189(5):1641–1647.

23. Sasoh M, Masai E, Ishibashi S, Hara H, Kamimura N, Miyauchi K, Fukuda M. Characterization of the terephthalate degradation genes of *Comamonas* sp. strain E6. *Appl Environ Microbiol.* 2006;72(3):1825–1832.
24. Kenny ST, Runic JN, Kaminsky W, Woods T, Babu RP, Keely CM, O’Connor KE. Up-cycling of PET (polyethylene terephthalate) to the biodegradable plastic PHA (polyhydroxyalkanoate). *Environ Sci Technol.* 2008;42(20):7696–7701.
25. Tiso R, Narancic R, Wei R, Pollet E, Beagan N, Schröder K, Honak A, Jiang M, Kenny ST, Wierckx N, et al. Bio-upcycling of polyethylene terephthalate. *bioRxiv.* Forthcoming 2020. <https://doi.org/10.1101/2020.03.16.993592>.
26. Altschul SF, Gish W, Miller W, Myers EW, Lipman DJ. Basic local alignment search tool. *J Molecul Biol.* 1990;215:403–410.
27. UniProt Consortium. Entry for TphB. 2019 [accessed 2020 Sep 29]. <https://www.uniprot.org/uniprot/Q5D0X4>.
28. Roell GW, Zha J, Carr RR, Koffas MA, Fong SS, Tang YJ. Engineering microbial consortia by division of labor. *Microb Cell Factories.* 2019;18(35).

List of Abbreviations

34dhbz	3,4-dihydroxybenzoate (protocatechuate)
acetyl-CoA	acetyl coenzyme A
ATP	adenosine triphosphate
BLAST	Basic Local Alignment Search Tool
COBRAPy	constraint-based reconstruction and analysis toolbox for Python
DCD	1,2-dihydroxy-3,5-cyclohexadiene-1,4-dicarboxylate
EG	ethylene glycol
FBA	flux balance analysis
GSMM	genome-scale metabolic model
MFS	major facilitator superfamily
NCBI	National Center for Biotechnology Information
PCA	protocatechuate (3,4-dihydroxybenzoate)
PET	polyethylene terephthalate
<i>P. putida</i>	<i>Pseudomonas putida</i>
SAMMIpy	semi-automated metabolic map illustrator in Python
TCA	tricarboxylic acid
TPA	terephthalic acid
TTT	tripartite tricarboxylate transporter

1 DEFENSE TECHNICAL
(PDF) INFORMATION CTR
DTIC OCA

1 CCDC ARL
(PDF) FCDD RLD DCI
TECH LIB

5 CCDC ARL
(PDF) FCDD RLS CB
AV TOBIAS
MA PERISIN
VE MARTINDALE
FCDD RL CL
JJ SUMNER
FCDD RLD D
PD COLLINS

1 OUSD(R&E)/RT&L
(PDF) EW KENT

1 HAMPTON UNIV
(PDF) L LEWIS